

# Compact four-mode silicon multimode bends with a 500 nm bandwidth

Feng Li

School of Information Science and Engineering

Yanshan University

Qinhuangdao, China

2074430750@qq.com

Fengyao Ding

School of Information Science and Engineering

Yanshan University

Qinhuangdao, China

3318447020@qq.com

Rui Wu

School of Information Science and Engineering

Yanshan University

Qinhuangdao, China

wurui@stumail.ysu.edu.cn

Yingjie Liu

School of Information Science and Engineering

Yanshan University

Qinhuangdao, China

liuyingjie@ysu.edu.cn

Ke Xu

Dept. of Electronic and Information Engineering

Harbin Institute of Technology

Shenzhen, China

kxu@hit.edu.cn

**Abstract**—A double-etch multimode bending based on four free-form curves is proposed. The designed device with an equivalent radius of only 14  $\mu\text{m}$  has low loss ( $<0.18$  dB) and crosstalk ( $<-20$  dB) over 500 nm bandwidth.

**Keywords**—silicon photonics, multimode bend, double-etching, photonic integrated circuits

## I. INTRODUCTION

To meet the exponentially increasing demand for large I/O bandwidth in optical interconnect system, on-chip multiplexing techniques is regarded as a promising solution to increase the data capacity. Mode division multiplexers (MDM) have multiple orthogonal guiding mode channels and is compatible with other multiplexing techniques to further increase data capacity, which has attracted much interests [1, 2]. The MDM technique avoids precise control of multi-wavelength laser source compared with wavelength division multiplexing and thus offers a low-cost solution for short-reach parallel data communications. Many multimode silicon photonics key building blocks for MDM systems have been extensively reported in recent years [3-6], such as mode (de) multiplexers, multimode waveguide crossing, multimode power splitter, multimode grating coupler, etc.

Multimode waveguide bending (MWB) plays an important role in on-chip MDM integrated circuits to help improve channel density, and many efforts have been devoted to the realization of sharp multimode bending [7-15]. In conventional MWB, the mode transmission loss and intermode crosstalk caused by mode mismatch between straight waveguide and curved waveguide are difficult to solve simultaneously at a small radius [7]. Great efforts have been made over the past few years to develop new structures for MWB. The ultra-compact MWB with a small radius ( $<4$   $\mu\text{m}$ ) is realized via digital meta-structure [8, 9]. However, the optimized parameters of these device are limited to the distribution of nanoholes, and it is difficult to further improve the performance. The MWB based on free curve is discretized by a series of circular arcs with different radii to better realize the MWB with the reasonable curvature radii in a small area and reduce propagation loss [10-12]. The structure with shallowly etched non-uniform subwavelength grating (SWG) has recently been introduced on the top surface of MWB [13, 14], which is used to spatially modify the refractive index profile in the multimode bent section. In

this way, the mode profiles in the multimode bent section have very little mode mismatch with those of the straight multimode waveguide. There are also proposed new ultra-sharp MWB based on multimode waveguide corner-bend (MWCBC) with total internal reflection (TIR). The device has a low insertion loss (IL) and low inter-mode crosstalk (CT) within a 400 nm operating bandwidth, but needs to maintain a wide waveguide size. Although a large number of optimization designs is used for MWB, it is still difficult to achieve high performance and ultrawide working bandwidth while maintaining a compact size.

In this paper, a double-etching MWB based on four free-form curves for supporting four modes ( $\text{TE}_0$ ,  $\text{TE}_1$ ,  $\text{TE}_2$  and  $\text{TE}_3$  modes) is proposed. Four freedom curves can greatly

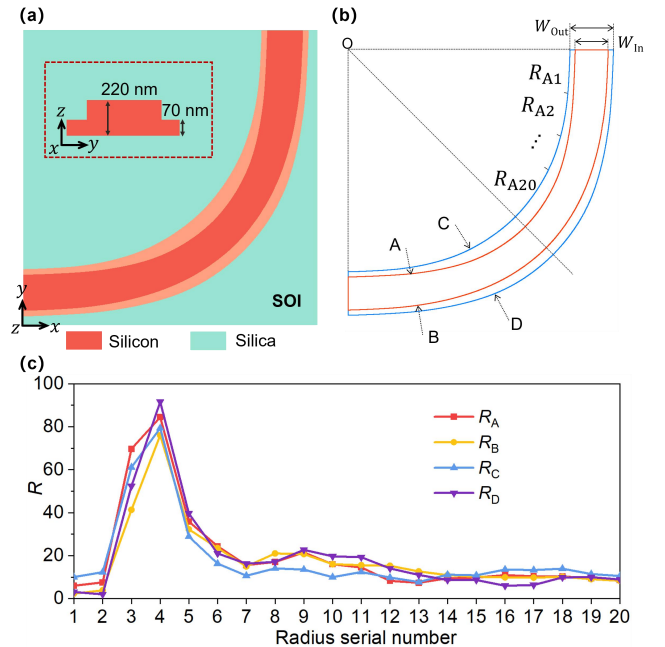


Fig. 1. (a) Schematic diagram of the designed four-mode MWB with two-step etching of 150 and 220 nm. (b) Top view of the designed four-mode MWB based on four degrees of freedom curves (A, B, C and D). (c) The optimized distributions of the segment radii for four-mode MWB with four degrees of freedom curves.

expand the optimization parameter space. The double-etching structure with shallow etching and full etching can

constrain light in different wavelength ranges, allowing DEMB to achieve greater bandwidth without significant loss and crosstalk, which can make MWB achieve larger bandwidth without serious loss and crosstalk. We numerically simulate the transmission properties of the designed device, and theoretically analyze the fabrication tolerance of the device. The simulation results show that the designed MWB has extremely low loss and low crosstalk from 1500 nm to 2000 nm.

## II. DEVICE DESIGN

The four-mode MWB is designed on 220 nm thick silicon-on-insulator (SOI) platform with two-step etching of 150 and 220 nm silicon (Si) layer and 2  $\mu\text{m}$  thick silica ( $\text{SiO}_2$ ) cladding, as shown in Fig. 1(a). Fig. 1(b) is top view of the designed four-mode MWB, which has an equivalent radius of 14  $\mu\text{m}$  and is composed of four free-form curves A, B, C and D duo to two-step etching. The width of the 220 nm full-etched waveguide ( $W_{\text{out}}$ ) is defined as 2.5  $\mu\text{m}$ , and the width of the 150 nm shallow-etched waveguide ( $W_{\text{in}}$ ) is defined as 1.9  $\mu\text{m}$ , which can support multimode operation and expand bandwidth. The 90° free-form curves are mirror-symmetrical along the 45° angular bisector, and the whole segment number is set as  $2N$  for all free-form curves. Here, each free-form curve of 45 degree bent waveguide is discretized into 20 different curvature radii, that is  $N=20$ .  $R_{Ai}$  is the curvature radius of the  $i$ -th arc for curve A. Similarly, there is the same definition for free-form curves B, C and D.

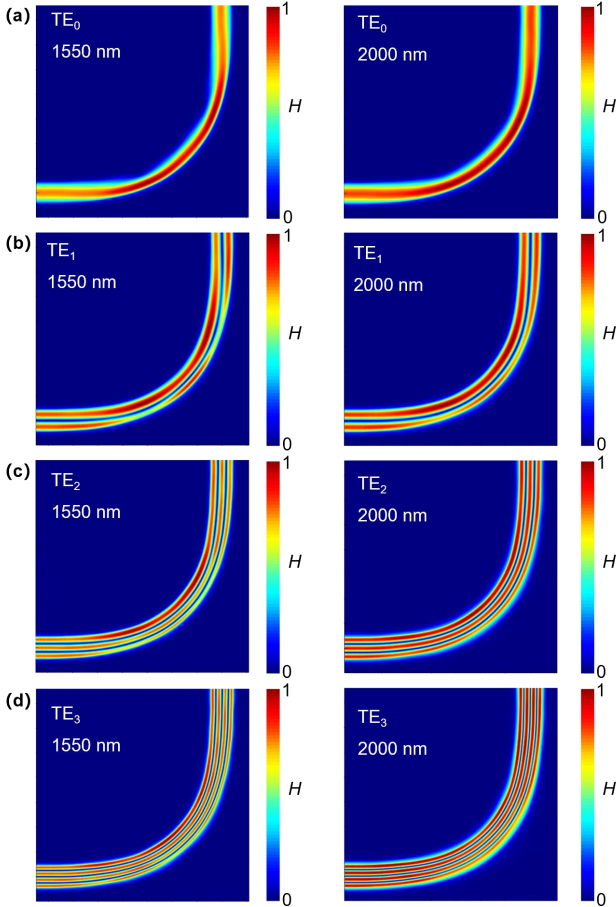


Fig. 2. The simulated optical field distributions of the designed MWB at 1550 nm and 2000 nm for (a)  $\text{TE}_0$  mode, (b)  $\text{TE}_1$  mode, (c)  $\text{TE}_2$  mode and (d)  $\text{TE}_3$  mode.

The performance of the proposed MWB is designed by optimizing distributions of 20 segment radii. The figure-of-merit (FOM) of the designed device is calculated via the three-dimensional finite difference time domain (3D FDTD) method by using Lumerical FDTD solution software. The value of FOM is related to the average ILs and CTs for four modes ( $\text{TE}_0$ ,  $\text{TE}_1$ ,  $\text{TE}_2$  and  $\text{TE}_3$  modes) within 500 nm wavelength range (from 1500 nm to 2000 nm).

$$\text{FOM} = 1 - \frac{1}{M} (1 - \alpha) \sum (1 - T_i) - \frac{1}{M} \beta \sum X_{ij} \quad (1)$$

Where  $T_i$  is the average IL of  $i$ -th mode,  $X_{ij}$  is the average CT of  $i$ -th mode to  $j$ -th mode ( $i=1, 2, 3, 4$ ,  $j=1, 2, 3, 4$ ,  $i \neq j$ ) within the 500 nm operating bandwidth,  $M$  is the number of supported modes ( $M=4$ ),  $\alpha$  and  $\beta$  are weight coefficients with a value from 0 to 1, which are utilized to achieve a tradeoff between ILs and CTs. The ideal FOM should be 1 at perfect operating performance. The four free form surfaces are sequentially optimized. The initial value is selected as the parameter of a conventional waveguide bending with 14- $\mu\text{m}$  radius. Taking  $R_A$  of free-form curve A as an example, in the optimization,  $R_{A1}$  is regarded as  $r_{A1}$ , and  $r_{A1}$  is traversed from  $0.5R_{A1}$  to  $1.5R_{A1}$  (defining 0.05 $R_{A1}$  per change). The FOM is calculated repeatedly for each new value of  $r_{A1}$ , so as to determine the optimized  $R_{A1}$ . One iteration ends up until  $R_{A1}$ - $R_{A20}$  are optimized according to this method. The program runs several iterations for four free curves until the objectives are met or the FOMs are not improved further. Fig. 1(c) shows the optimized distributions of the segment radii for four-mode MWB with four degrees of freedom curves. It can be seen that the radius variation trends of the four curves are similar. The curvature radius of the first arc to the fourth arc increases rapidly, and the curvature radius of the fourth arc reaches the peak. The curvature radius after the fourth arc is irregularly reduced to shrink the overall bending radius. The optimization process takes  $\sim 120$  hours to get the convergent results after three iterations using an 8-core desktop.

## III. DEVICE SIMULATION AND DISCUSSION

To evaluate the performance of the optimized wavelength demultiplexer, the optical field distribution is numerically calculated using 3D FDTD simulation. Fig. 2 shows the magnetic field distribution ( $H$  field) of the designed MWB at

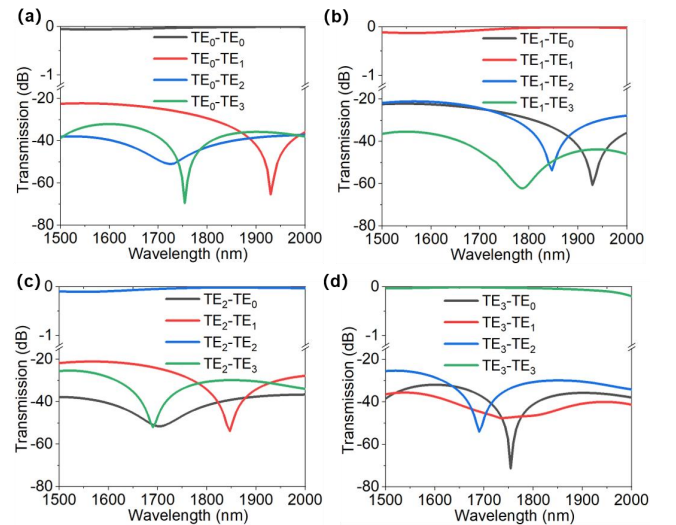


Fig. 3. The simulated transmission spectra of the designed MWB from 1500 nm to 2000 nm for (a)  $\text{TE}_0$  mode, (b)  $\text{TE}_1$  mode, (c)  $\text{TE}_2$  mode and (d)  $\text{TE}_3$  mode.

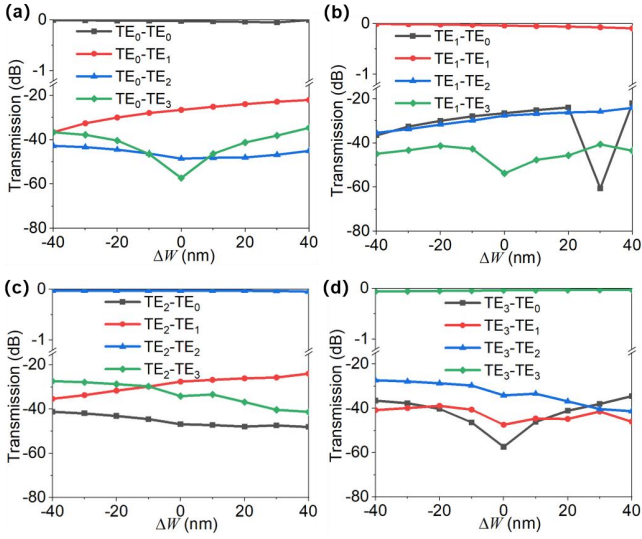


Fig. 4. The simulated transmission of the designed MWB at 1750 nm for (a) TE<sub>0</sub> mode, (b) TE<sub>1</sub> mode, (c) TE<sub>2</sub> mode and (d) TE<sub>3</sub> mode.

1550 nm and 2000 nm for TE<sub>0</sub>, TE<sub>1</sub>, TE<sub>2</sub> and TE<sub>3</sub> modes, respectively. It can be seen that the optical waves for all the modes are transmitted from the input port, pass through the designed MWB, and reach the output port smoothly. The output modes maintain very high mode purity with negligible mode conversion to other order modes in transmission process. It can also be noted that all modes are well propagating without obvious leakage at different wavelengths.

We also quantitatively study the ILs and CTs of the designed MWB. Fig. 3 is the numerically calculated transmission spectra for all modes in the wavelength range of 1500 nm to 2000 nm. It can be seen that the simulated ILs for TE<sub>0</sub>-TE<sub>3</sub> modes are lower than 0.18 dB over 500 nm bandwidth, and the inter-mode CTs are lower than -20 dB within the whole working bandwidth.

To further determine the performance of the proposed device, the fabrication tolerance is analyzed by using the 3D FDTD method. Fig. 4 shows the IL and CT changes of the designed MWB for all modes at the center wavelength (1750 nm) under the fabrication error of -40 nm to 40 nm. It can be seen that the transmission loss variations for TE<sub>0</sub>-TE<sub>3</sub> modes are maintained within 0.1 dB. And the CTs can be maintained < -20 dB in the error range of -40 nm to 40 nm. The simulation results show that the designed MWB has a large fabrication tolerance with  $\pm 40$  nm.

#### IV. CONCLUSION

In conclusion, we have proposed a compact and multimode bends with double-etching and four free-form

curves for supporting TE<sub>0</sub>-TE<sub>3</sub> modes. The designed device has high transmission performance (IL < 0.18 dB and CT < -20 dB) and large fabrication tolerance ( $\geq \pm 40$  nm) over 500 nm bandwidth. The proposed MWB can play an important role in on-chip multi-band and high-density integrated MDM transmission systems.

#### ACKNOWLEDGMENT

This work is supported by National Natural Science Foundation of China (NSFC) (U21A20454), Shenzhen Science and Technology Innovation Commission (RCYX20210609103707009), Natural Science Foundation of Guangdong Province for Distinguished Young Scholars (2022B1515020057).

#### REFERENCES

- [1] R. B. Priti, O. Liboiron-Ladouceur, "Reconfigurable and scalable multimode silicon photonics switch for energy-efficient mode-division-multiplexing systems," *J. Lightwave Technol.*, vol. 37, pp. 3851-3860, 2019.
- [2] X. Zheng et al., "Silicon-based four-mode division multiplexing for chip-scale optical data transmission in the 2  $\mu$ m waveband," *Photon. Res.*, vol. 7, pp. 1030-1035, 2019.
- [3] C. Li, D. Liu, D. Dai, "Multimode silicon photonics," *Nanophotonics*, vol. 8, pp. 227-247, 2019.
- [4] C. Sun et al., "Key multimode silicon photonic devices inspired by geometrical optics," *ACS. Photon.*, vol. 7, pp. 2037-2045, 2020.
- [5] X. Zhou, H. K. Tsang, "High efficiency multimode waveguide grating coupler for few-mode fibers," *IEEE Photon. J.*, vol. 14, pp. 1-5, 2022.
- [6] X. Guo et al., "Ultra-broadband multimode waveguide crossing via subwavelength transmittarray with bound state," *Laser Photon. Rev.*, 2200674, 2023.
- [7] S. Li et al., "Compact and broadband multimode waveguide bend by shape-optimizing with transformation optics," *Photon. Res.*, vol. 8, pp. 1843-1849, 2020.
- [8] Y. Liu et al., "Very sharp adiabatic bends based on an inverse design," *Opt. Lett.*, vol. 43, pp. 2482-2485, 2018.
- [9] Y. Liu et al., "Arbitrarily routed mode-division multiplexed photonic circuits for dense integration," *Nat. Commun.*, vol. 10, pp. 3263, 2019.
- [10] M. Bahadori et al., "Universal design of waveguide bends in silicon-on-insulator photonics platform," *J. Lightwave Technol.*, vol. 37, pp. 3044-3054, 2019.
- [11] S. Sun et al., "Ultra-sharp silicon multimode waveguide bends based on double free-form curves," *Photon. Res.*, vol. 10, pp. 1484-1490, 2022.
- [12] S. Sun et al., "Inverse design of ultra-compact multimode waveguide bends based on the free-form curves," *Laser Photon. Rev.*, vol. 15, pp. 2100162, 2021.
- [13] H. Wu et al., "Ultra-sharp multimode waveguide bends with subwavelength gratings," *Laser Photon. Rev.*, vol. 13, pp. 1800119, 2019.
- [14] S. Gao, H. Wang, X. Yi, C. Qiu, "Ultra-compact multimode waveguide bend with shallowly etched grooves," *Opt. Express*, vol. 29, pp. 38683-38690, 2021.
- [15] Y. Wang, D. Dai, "Multimode silicon photonic waveguide corner-bend," *Opt. Express*, vol. 28, pp. 9062-9071, 2020.